Phase diagrams of mixtures of flexible polymers and nematic liquid crystals in a field

Zhiqun Lin,[1] Hongdong Zhang,[1] and Yuliang Yang[1,2,*]

[1]*Laboratory of Macromolecular Engineering of Polymers, Department of Macromolecular Science, Fudan University,
Shanghai 200433, China*
[2]*Institute of Chemistry, Chinese Academy of Science, Beijing 100080, China*

The Flory-Huggins theory of flexible polymers mixtures [P. J. Flory, *Principles of Polymer Chemistry* (Cornell University Press, Ithaca, 1953)] and the Lebwohl-Lasher model of nematogens [G. Lasher, Phys. Rev. A **5**, 1350 (1972); P. A. Lebwohl and G. Lasher, *ibid.* **6**, 426 (1972)] are combined to understand the phase behaviors of mixtures of flexible polymers (coils) and small molecular liquid crystals in an external magnetic field. It is found that, due to the field-induced ordering, the phase boundaries shift upwards and the paranematic spinodal regions are narrowed near the paranematic-nematic transition lines; however, the nematic spinodal regions are enlarged. [S1063-651X(98)13110-0]

PACS number(s): 61.30.−v, 61.41.+e, 64.60.Cn

I. INTRODUCTION

Phase transitions in an external field have been of interest for a long time. The behavior of a nematic bulk liquid crystal (LC) in the presence of an external field is of importance for many technical applications as well as basic physical research. In the framework of the Maier-Saupe model [1], Wojtowicz and Sheng have developed a mean field theory to examine the effects of an external magnetic field on the nematic-isotropic (N-I) transition of nematic LCs [2]. It is found that the field-temperature phase diagram exhibits a line of first-order transitions that terminates at a classical critical point. Very recently, Seidin, Mukamel, and Allender have studied the phase diagram of cholesteric LCs in a field [3]. They found that the temperature-field phase diagram is strongly dependent on the intrinsic chirality when the applied field direction is perpendicular to the pitch axis. In this work we investigate the phase behaviors of the mixtures of flexible polymers (coils) and nematic LCs in an external applied field in the context of phase equilibrium between a coil and a nematic LC and the phase transition between nematic and isotropic states.

The phase equilibrium in the mixtures of coils and LCs is related to the composites materials of polymers and small molecular LCs, which are often called polymer dispersed liquid crystals (PDLCs). Various PDLC materials have been studied for their potential applications, in particular the privacy windows and devices operating on the principle of electrically controlled light scattering [4–8]. The PDLC materials are usually prepared by thermal induced phase separation [9,10] or polymerization induced phase separation [11]. In experiment, external magnetic or electric fields have been applied during the phase separation process in order to obtain the desired overall director orientation in the PDLC film and to achieve higher optical contrast between off and on states [12]. As a matter of fact, questions are raised with the introduction of an external field, i.e., the external field effects on

the phase equilibrium coils and LCs, the N-I transition, and the spinodal transition. These are the main problems we will tackle in this paper.

II. MODEL

In order to predict theoretically the phase diagrams of the system, based on the Flory-Huggins model [13] for an isotropic polymer solution and the Lebwohl-Lasher model [14,15] for nematogens, the statistical thermodynamics theory for the system of coils and LCs has been developed in our previous work [16,17]. It is shown that this theory agrees with the experimental results quite well [18,19]. The free-energy functional derived in Refs. [16,17] also has been successfully applied to the time-dependent Ginzburg-Landau model to predict the spinodal decomposition dynamics of the coil-LC mixtures in the early stage [20].

Following the same procedure of our previous papers [16,17], in the mean field framework, the potential of an anisotropic interaction between nematogens in a system with LC volume fraction φ_L and an external magnetic field **H** applied to nematogenic molecules having the positive diamagnetic anisotropy $\Delta\chi = \chi_\parallel - \chi_\perp$ can be written as

$$\frac{V}{kT} = -\frac{z\varphi_L\epsilon_{LL}}{kT}P_2(\cos\theta)S(\varphi_L) - \frac{\Delta\chi}{kT}(\mathbf{n}\cdot\mathbf{H})^2$$

$$\equiv -\chi_{LL}\varphi_L S(\varphi_L)P_2(\cos\theta) - \chi_h\cos^2\theta, \qquad (1)$$

where $\chi_{LL} = z\epsilon_{LL}/kT$, z is the coordination number ($z = 6$ for the cubic lattice), ϵ_{LL} is the maximum interaction energy between LC molecules, $\chi_h = \Delta\chi H^2/kT$, $P_2(\cos\theta)$ is the second Legendre function, and $S(\varphi_L)$ is the orientation order parameter of the LC with volume fraction φ_L. We should note that the potential given in Eq. (1) is the same as that used by Wojtowicz and Sheng [2]. The temperature, interaction energy, composition, and field strength dependence of $S(\varphi_L)$ is given by the self-consistent equation

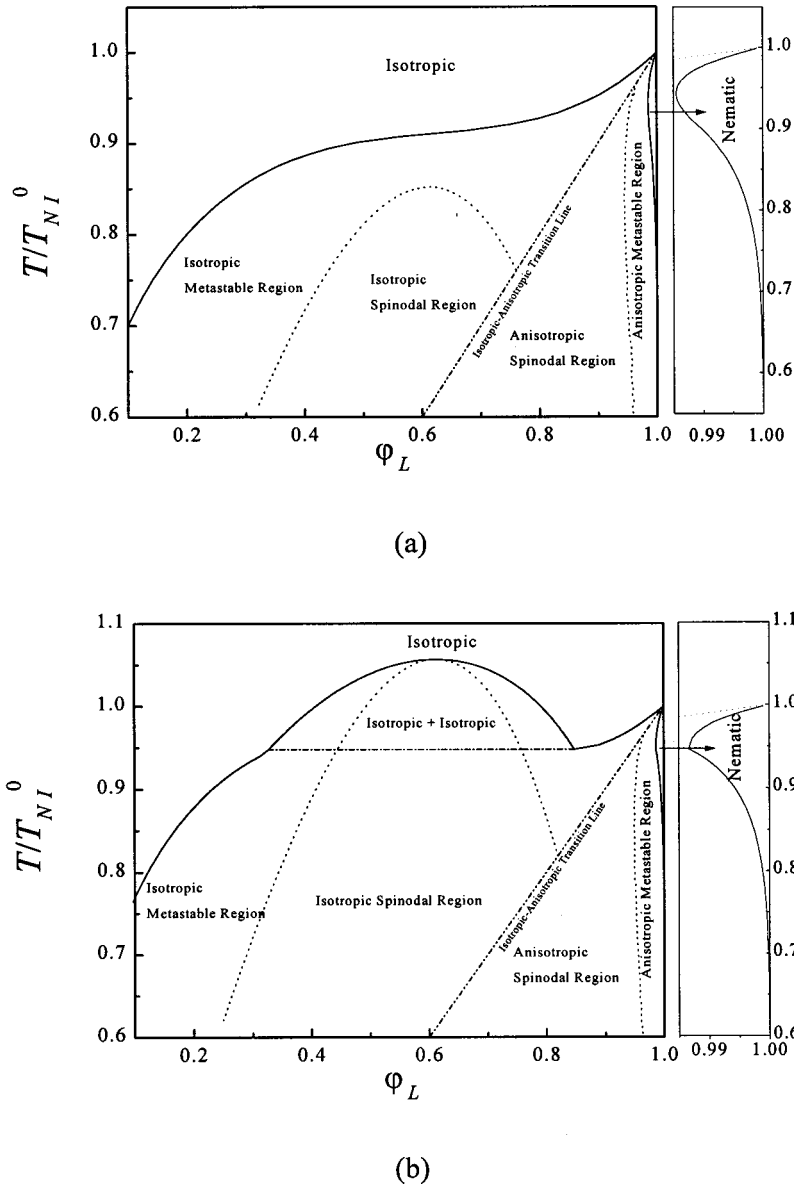*Author to whom correspondence should be addressed.

(a)

(b)

FIG. 1. Phase diagrams and the spinodal lines of coil-LC binary mixtures in the absence of an external field. (a) $x_p = 2.5$, $T_{NI}^0 = 308.05$ K, and $\chi_{LP} = 349.71 - 0.0001/T$. (b) $x_P = 4.5$ and the other parameters are the same as in (a). It can be seen that the isotropic-isotropic coexistent region emerges when the chain length is increased. The same situation will happen if the Flory-Huggins interaction parameter χ_{LP} is increased.

$$S(\varphi_L) = \frac{1}{Z(\varphi_L)} \int_0^1 d \cos \theta P_2(\cos \theta) \exp(-V/kT). \quad (2)$$

The partition function for LCs in the coil-LC mixture is written as

$$Z(\varphi_L) = \int_0^1 d \cos \theta \exp(-V/kT). \quad (3)$$

Following our previous papers [17,19], the free energy of the coils-LC mixtures in an external magnetic field is finally written as

$$\frac{F}{NkT} = \varphi_L \ln \varphi_L + \frac{1 - \varphi_L}{x_P} \ln(1 - \varphi_L) + \chi_{LP} \varphi_L (1 - \varphi_L)$$

$$+ \frac{1}{2} \varphi_L \left\{ \chi_{LL} \varphi_L S^2(\varphi_L) + \chi_h \frac{2S(\varphi_L) + 1}{3} \right\}$$

$$- \varphi_L \ln Z(\varphi_L), \quad (4)$$

where $\chi_{LP} = z\epsilon_{LP}/kT$ and ϵ_{LP} is the isotropic interaction energy between the coil segment and the nematogen. In obtaining Eq. (4) we have assumed that the polymer segments are magnetically isotropic.

Based on the above free energy, the phase equilibrium equations can be obtained by equating the chemical potentials of coils and LCs in two phases, i.e., $\Delta\mu_{L1} = \Delta\mu_{L2}$ and $\Delta\mu_{P1} = \Delta\mu_{P2}$. We arrive at
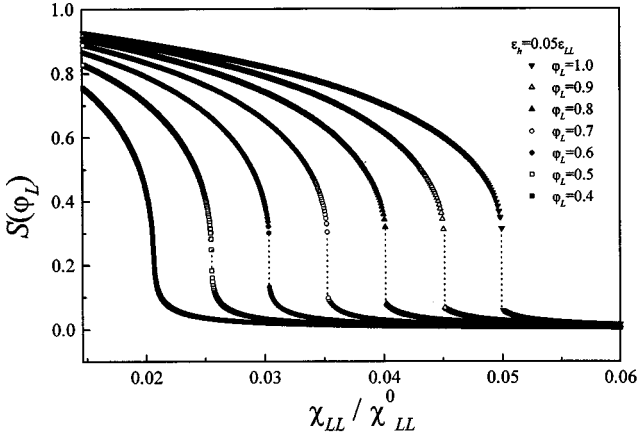
(a)
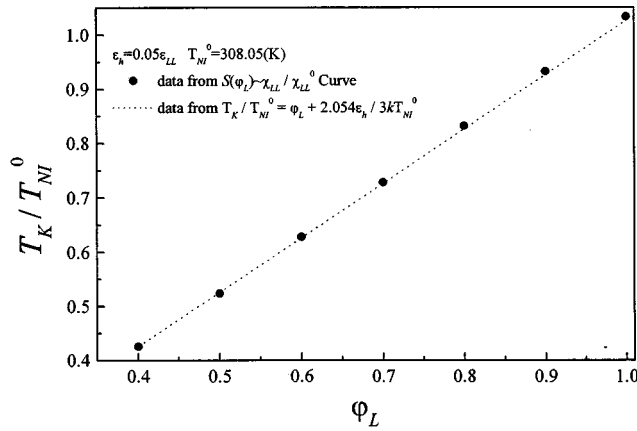
(b)

FIG. 2. (a) Order parameter $S(\varphi_L)$ vs χ_{LL} for various LC concentrations φ_L. The strength of the external magnetic field is set to $\varepsilon_h = 0.05\varepsilon_{LL}$. It can be seen that the nematic phase transforms into the paranematic phase with field-induced order and the order parameter in the paranematic phase near the right-hand side of the discontinuity is higher. (b) Nematic-paranematic transition temperature vs the LC concentration. The solid circles are the data from (a) and the dotted line is calculated from Eq. (10).

$$\ln\frac{\varphi_{L1}}{\varphi_{L2}} + \frac{1}{x_P}(\varphi_{L1} - \varphi_{L2})$$

$$+ \chi_{LP}(\varphi_{L1}^2 - \varphi_{L2}^2) - 2\chi_{LP}(\varphi_{L1} - \varphi_{L2})$$

$$+ \frac{1}{2}\chi_{LL}[\varphi_{L1}^2 S^2(\varphi_{L1}) - \varphi_{L2}^2 S^2(\varphi_{L2})]$$

$$+ \frac{\chi_h}{3}[S(\varphi_{L1}) - S(\varphi_{L1})]$$

$$+ \frac{\chi_h}{3}\left[\varphi_{L1}(1-\varphi_{L1})\frac{\partial S(\varphi_{L1})}{\partial\varphi_{L1}}\right.$$

$$\left. - \varphi_{L2}(1-\varphi_{L2})\frac{\partial S(\varphi_{L2})}{\partial\varphi_{L2}}\right]$$

$$- [\ln Z(\varphi_{L1}) - \ln Z(\varphi_{L2})] = 0 \qquad (5)$$

and

$$\frac{1}{x_P}\ln\frac{1-\varphi_{L1}}{1-\varphi_{L2}} + \left(\frac{1}{x_P}-1\right)(\varphi_{L1} - \varphi_{L2})$$

$$+ \chi_{LP}(\varphi_{L1}^2 - \varphi_{L2}^2)$$

$$+ \frac{1}{2}\chi_{LL}[\varphi_{L1}^2 S^2(\varphi_{L1}) - \varphi_{L2}^2 S^2(\varphi_{L2})]$$

$$- \frac{\chi_h}{3}\left[\varphi_{L1}^2\frac{\partial S(\varphi_{L1})}{\partial\varphi_{L1}} - \varphi_{L2}^2\frac{\partial S(\varphi_{L2})}{\partial\varphi_{L2}}\right] = 0. \qquad (6)$$

According to the definition of the spinodal curve, by setting the second derivatives of free energy equal to zero, we get

$$\frac{1}{2}\left(\frac{1}{\varphi_L} + \frac{1}{x_P(1-\varphi_L)}\right)$$

$$= \chi_{LP} - \frac{1}{2}\chi_{LL}S^2(\varphi_L) - 2\chi_{LL}\varphi_L S(\varphi_L)\frac{\partial S(\varphi_L)}{\partial\varphi_L}$$

$$- \frac{1}{2}\chi_{LL}\varphi_L^2\left(\frac{\partial S(\varphi_L)}{\partial\varphi_L}\right)^2$$

$$- \frac{1}{2}\chi_{LL}\varphi_L^2 S(\varphi_L)\frac{\partial^2 S(\varphi_{L1})}{\partial\varphi_L^2} - \frac{\chi_h}{3}\frac{\partial S(\varphi_L)}{\partial\varphi_{L1}}$$

$$- \frac{\chi_h}{6}\varphi_L\frac{\partial^2 S(\varphi_L)}{\partial\varphi_L^2} + \frac{\partial\ln Z(\varphi_L)}{\partial\varphi_L}$$

$$+ \frac{1}{2}\varphi_L\frac{\partial^2\ln Z(\varphi_L)}{\partial\varphi_L^2}. \qquad (7)$$

The phase diagrams comprising the spinodal curves are calculated by numerically solving Eqs. (5)–(7). In the numerical calculation, we assume that the N-I transition temperature in the absence of external field is $T_{NI}^0 = 308.05$ K (i.e., $\chi_{LL}^0 = z\varepsilon_{LL}/kT_{NI}^0 = 4.541$), which corresponds to the case of 4′-pentyl-4-biphenyl carbonitrile [16].

III. MEAN FIELD PHASE DIAGRAMS

For clarity, we present the typical phase diagrams in the absence of an external field. Figure 1 shows the phase diagrams and the spinodal lines of coil-LC binary mixtures in the absence of an external field. It is seen that the phase diagrams are highly asymmetric and there exists a narrow nematic phase region when the LC concentration φ_L is high. The nematic region becomes narrower as the chain length x_P or the Flory-Huggins interaction parameter χ_{LP} is increased. Therefore, in order to make the nematic phase region visible, we present only the phase diagrams of short chain lengths in this paper. Comparing the phase diagrams of Figs. 1(a) and 1(b), it can be seen that the classic isotropic-isotropic (I + I) coexistent region emerges in Fig. 1(b) when χ_{LP} and/or x_P is increased. More interestingly, there are two spinodal regions (unstable regions) in the phase diagrams, i.e., an isotropic spinodal region and a nematic spinodal region, which are separated by a N-I transition line. It is known from the linear kinetic analysis that the spinodal decomposition be-
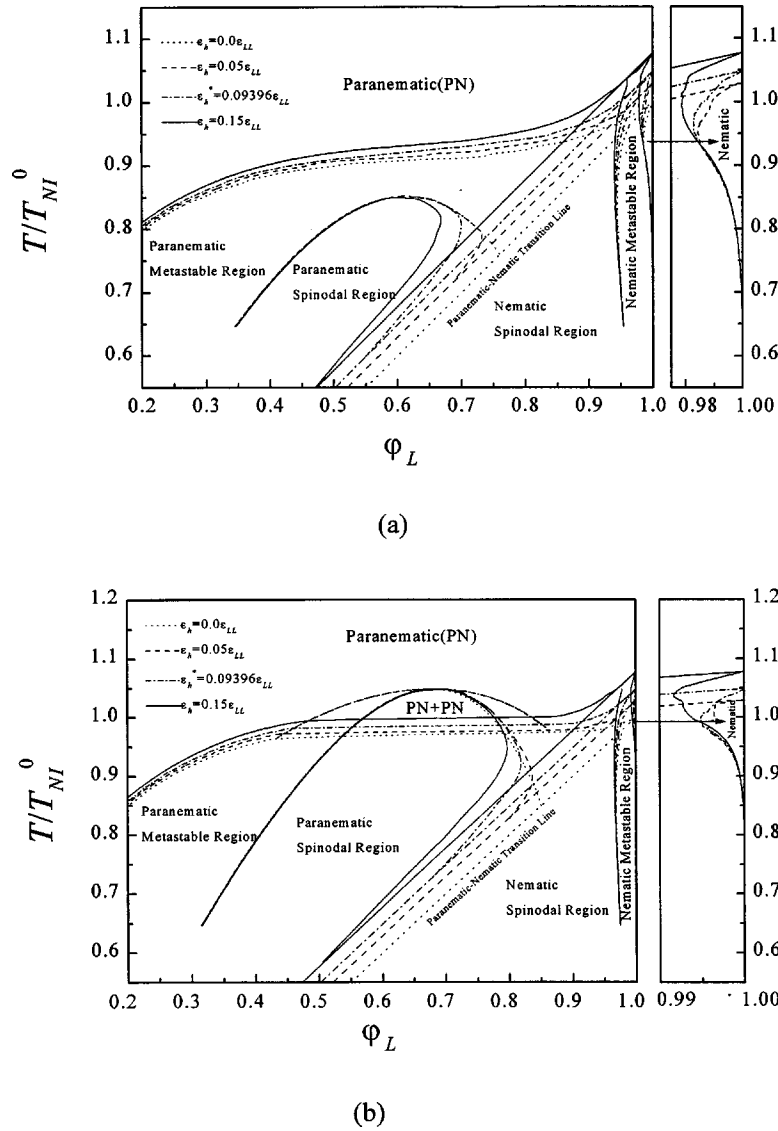
(a)

(b)

FIG. 3. Phase diagram together with the spinodal lines of coil-LC mixtures in an external magnetic field. (a) The corresponding parameters used in the calculation are the same as those in Fig. 1(a). (b) The corresponding parameters used in the calculation are same as those in Fig. 1(b). The strengths of the external magnetic field used in the calculations are given in the insets. For the sake of comparison, the phase diagrams and the spinodal lines in the absence of the external field are also given as dotted lines.

haviors in the isotropic and anisotropic spinodal regions are quite different [20].

Certainly, the phase diagrams in an external field is more complicated. Even for a bulk LC, Wojtowicz and Sheng [2] have shown that, in the presence of an external field, the bulk LC transition temperature T_K linearly increases with the increasing strength of the external magnetic field

$$T_K = T_{NI}^0 + 1.0270 \frac{2\varepsilon_h}{3k}, \qquad (8)$$

where T_{NI}^0 is the transition temperature of the bulk LC in the absence of an external field and $\varepsilon_h = \Delta\chi H^2$. We designate the transition temperature as T_K because in the presence of an external magnetic field the order parameter S is nonzero and the state is paranematic (PN) instead of isotropic when

the temperature is higher than T_K. Therefore, T_K is the equilibrium temperature between N and PN states. We have shown in our previous work that [16] in the coil-LC with system a LC concentration of φ_L, the composition dependence of T_{NI} in the absence of an external field has the relation $T_{NI} = \varphi_L T_{NI}^0$. Combining with the results of Eq. (8), we have

$$T_K = \varphi_L T_{NI}^0 + 1.0270 \frac{2\varepsilon_h}{3k}. \qquad (9)$$

Equation (9) can be rewritten as

$$T_K / T_{NI}^0 = \varphi_L + 1.0270 \frac{2\varepsilon_h}{3k T_{NI}^0}, \qquad (10)$$

i.e., the transition temperature T_K increases linearly with increasing φ_L and/or ε_h. Equation (10) is confirmed by the results calculated from Eq. (2) shown in Fig. 2. We must mention that in the PN phase, the order parameter S is higher when the system is close to the N-PN transition line. This behavior affecting the spinodal lines in the phase diagrams will be seen in the following.

Now we turn to the discussion of the mean field phase diagrams in the presence of an external magnetic field. In the presence of an external magnetic field, the phase diagrams shown in Fig. 3 are calculated by solving Eqs. (5) and (6). In Fig. 3 the N-PN transition lines under the different strengths of the external magnetic fields are calculated from Eq. (10). It is seen from Fig. 3 that the $N+$PN coexistent phase boundary, which corresponds to the $N+I$ coexistent biphasic phase boundary in Fig. 1, shifts upward with the increasing strength of the external field. The PN$+$PN coexistent biphasic boundary, which corresponds to the $I+I$ coexistent phase boundary in Fig. 1(b), is almost unaffected by the external magnetic field as this region is relatively far away from the N-PN transition line and thus the order parameter S in this region is low. However, due to the increase of the $N+$PN coexistent biphasic boundary, the PN$+$PN biphasic region becomes smaller as the strength of the external field is increased. It is expected that, eventually, the PN$+$PN coexistent region disappears when the strength of the external magnetic field is strong enough.

It also can be seen from Fig. 3 that the N-PN phase transition line, which corresponds to the N-I transition line in Fig. 1, shifts upward with increasing strength of the external magnetic field. This phenomenon can be easily understood from Eq. (10).

IV. SPINODAL LINES IN AN EXTERNAL MAGNETIC FIELD

The spinodal lines shown in Fig. 3 are calculated from Eq. (7). We should mention also that the spinodal region on the left-hand side of the N-PN transition line defined by Eq. (10) is now the PN-spinodal region, which corresponds to the I-spinodal region in Fig. 1. It is interesting to note that the PN-spinodal line is strongly dependent on the strength of the external magnetic field. The PN-spinodal region near the N-PN transition line is narrowed because the order parameter S of the PN phase is nonzero and higher when the system is close to the N-PN transition line. Therefore, this narrowing effect is more severe when the strength of the external magnetic field is higher.

On the other hand, the spinodal region on the right-hand side of N-PN transition line defined by Eq. (10) is the N-spinodal region. It can be seen from Fig. 3 that the N-spinodal region is broadened. This is also due to the fact that, in the presence of an external magnetic field, the order parameter S in the nematic phase is higher than the value in the absence of an external field.

V. CONCLUSIONS

In this paper the phase diagrams of coil-LCs binary mixtures in an external magnetic field are calculated. It is found that in the presence of an external magnetic field, the N phase with higher S transforms into the PN phase with lesser field-induced order S. The N-PN phase transition temperature T_K of the bulk LC increases with the increasing strength of the external magnetic field. In the mixtures of coils and LCs, the transition temperature T_K increases linearly with the increasing φ_L and Eq. (10) follows.

Due to the effect of field-induced ordering, the driving force for the phase separation is enhanced and results in the $N+$PN coexistent region shifting upward and broadening. In the PN$+$PN coexistent region, where the field-induced ordering is weak, it is almost unaltered by the external magnetic field.

It is also found that there are two spinodal regions in the phase diagram, i.e., the PN-spinodal region and the N-spinodal region. The PN-spinodal region near the left-hand side of the N-PN transition line is narrowed because the field-induced order parameter S of the PN phase is higher, which stabilizes the ordered phase. However, the same effect will stabilize the N phase and cause the broadening of the N-spinodal region.

Although no comparison between experimental results and our theoretical results has been made due to the lack of experimental data, we believe that the theoretical results obtained in this work are meaningful for both the condensed state physics of the system containing LCs and the preparation of polymer dispersed LC materials.

[1] W. Maier and A. Saupe, Z. Naturforsch. A **13**, 564 (1958); **15**, 287 (1960).

[2] P. J. Wojtowicz and P. Sheng, Phys. Lett. **48A**, 253 (1974).

[3] R. Seidin, D. Mukamel, and D. W. Allender, Phys. Rev. E **56**, 1773 (1997).

[4] J. W. Doane *et al.*, Appl. Phys. Lett. **48**, 269 (1986).

[5] P. S. Drazaic, J. Appl. Phys. **60**, 2142 (1986).

[6] G. Chidichimo, G. Arabia, and A. Golemme, Liq. Cryst. **5**, 1443 (1989).

[7] C. Cipparrone *et al.*, Mol. Cryst. Liq. Cryst. **179**, 269 (1990).

[8] Y. K. Fung, D. K. Yang, and J. W. Doane, Proc. SPIE **1664**, 41 (1992).

[9] T. Kajiyama, A. Miyamoto, H. Kikuchi, and Y. Morimura, Chem. Lett. **1989**, 813.

[10] J. W. Doane, *Liquid Crystals, Their Application and Uses*, edited by B. Bahadur (World Scientific, Teaneck, 1990), Chap. 14.

[11] J. Y. Kim and P. Palffy Muhoray, Mol. Cryst. Liq. Cryst. **203**, 93 (1991).

[12] Paul S. Drzaic, Proc. SPIE **1080**, 11 (1989).

[13] P. J. Flory, *Principles of Polymer Chemistry* (Cornell University Press, Ithaca, 1953).

[14] G. Lasher, Phys. Rev. A **5**, 1350 (1972).

[15] P. A. Lebwohl and G. Lasher, Phys. Rev. A **6**, 426 (1972).

[16] Y. Yang, J. Lu, H. Zhang, and T. Yu, Polym. J. (Tokyo) **26**, 880 (1994).

[17] H. Zhang, F. Li, and Y. Yang, Sci. China B **38**, 412 (1995).

[18] C. Shen and T. Kyu, J. Chem. Phys. **102**, 556 (1995).

[19] H. Zhang, Z. Lin, D. Yan, and Y. Yang, Sci. China B **40**, 128 (1997).

[20] Z. Lin, H. Zhang, and Y. Yang, Macromol. Theory Simul. **6**, 1153 (1997).